

RESEARCH ARTICLE

Ammonia Affects Astroglial Proliferation in Culture

Guillermo Bodega^{1*}, Berta Segura², Sergio Ciordia³, María del Carmen Mena³, Luis Andrés López-Fernández⁴, María Isabel García⁴, Isabel Trabado⁵, Isabel Suárez¹

1 Departamento de Biomedicina y Biotecnología, Universidad de Alcalá, 28871 Alcalá de Henares, Madrid, Spain, **2** Instituto de Salud Carlos III, UFIEC, Unidad de Neuro-Oncología, 28220 Majadahonda, Madrid, Spain, **3** Proteomics, Centro Nacional de Biotecnología/CSIC, Campus de Cantoblanco, Madrid, Spain, **4** Servicio de Farmacia, Instituto de Investigación Sanitaria Gregorio Marañón, Hospital General Universitario Gregorio Marañón, Madrid, Spain, **5** Unidad de Cultivos, Facultad de Medicina, Universidad de Alcalá, 28871 Alcalá de Henares, Madrid, Spain

* guillermo.bodega@uah.es



Abstract

Primary cultures of rat astroglial cells were exposed to 1, 3 and 5 mM NH₄Cl for up to 10 days. Dose- and time-dependent reductions in cell numbers were seen, plus an increase in the proportion of cells in the S phase. The DNA content was reduced in the treated cells, and BrdU incorporation diminished. However, neither ammonia nor ammonia plus glutamine had any effect on DNA polymerase activity. iTRAQ analysis showed that exposure to ammonia induced a significant reduction in histone and heterochromatin protein 1 expression. A reduction in cell viability was also noted. The ammonia-induced reduction of proliferative activity in these cultured astroglial cells seems to be due to a delay in the completion of the S phase provoked by the inhibition of chromatin protein synthesis.

OPEN ACCESS

Citation: Bodega G, Segura B, Ciordia S, Mena MdC, López-Fernández LA, García MI, et al. (2015) Ammonia Affects Astroglial Proliferation in Culture. PLoS ONE 10(9): e0139619. doi:10.1371/journal.pone.0139619

Editor: Shama Ahmad, University of Alabama at Birmingham, UNITED STATES

Received: May 22, 2015

Accepted: September 14, 2015

Published: September 30, 2015

Copyright: © 2015 Bodega et al. This is an open access article distributed under the terms of the [Creative Commons Attribution License](https://creativecommons.org/licenses/by/4.0/), which permits unrestricted use, distribution, and reproduction in any medium, provided the original author and source are credited.

Data Availability Statement: All relevant data are within the paper.

Funding: Support was provided by Universidad de Alcalá E02. The funder had no role in study design, data collection and analysis, decision to publish, or preparation of the manuscript.

Competing Interests: The authors have declared that no competing interests exist.

Introduction

Metabolic ammonia is the main causal agent of hepatic encephalopathy (HE) [1]. It has been suggested that ammonia might affect cerebral energy metabolism, neurotransmitter pathways, nitric oxide synthesis and signal transduction, and produce oxidative stress [2–4], but the exact pathological mechanisms underlying HE remain unknown.

Astroglial cells play a pivotal role in ammonia metabolism [5]. In fact, glutamine synthetase, the enzyme that detoxifies ammonia by condensing it with glutamate to form glutamine, is mainly found in astrocytes [6]. Astroglial dysfunction might, therefore, lead to nerve cell disease [7]. Many astroglial abnormalities have been reported in HE and hyperammonemia, with astroglial edema among the most prominent [8]. The effects of ammonia on astroglial proliferation, however, have been little documented. The many changes in cell physiology induced by ammonia might have an effect on the cell cycle (which is normally carefully regulated), and consequently on astroglial proliferation. However, it must be remembered that cell proliferation is reduced in this system in adult animals, even though the central nervous system possesses neural progenitor cells. *In vivo* studies showing ammonia-induced alterations of

astroglial proliferative activity are very scarce [9, 10], but they suggest that proliferation is increased.

In our work on the role of astrocytes in HE, we use astroglial cell cultures as an *in vitro* model. In routine monitoring of these cultures it was noticed that, at confluence, the cells continued to proliferate, but were smaller. Ammonia-treated astroglial cells, however, showed no similar size reduction, perhaps because of a potentially lower proliferation rate. The aim of the present work was therefore to examine the effect of ammonia on the proliferative activity of cultivated astroglial cells. In order to determine when the effect(s) of ammonia occur, the proportions of cells in different phases of the cell cycle were noted, and BrdU incorporation and chromatin protein expression investigated.

Materials and Methods

P0-P1 rats were anaesthetized with halothane to avoid unnecessary suffering and, after decapitation, the cerebral hemispheres dissected out. Astroglial cells, obtained as previously described [11], were grown in 75 cm² flasks (primary cultures) containing DMEM medium (Gibco) supplemented with 10% fetal bovine serum (FBS) (Gibco) and an antibiotic/antimycotic solution (Gibco), at 37°C in a 5% CO₂ atmosphere. Before confluence, the cells were detached with trypsin and reseeded (forming secondary cultures) in different multiwell plates (6, 24 and 96 wells) with FBS concentrations depending on the experiment (see below). The Wistar rats used to provide the astroglial cells were handled adhering to European Union Directive 63/2010/EC, Spanish law (Real Decreto 53/2013), and institutional guidelines on animal welfare prepared by the “Comité de Ética de Investigación y Experimentación Animal (Universidad de Alcalá)”. This study was approved by this committee and the sacrifice of the rats performed under its supervision.

Hyperammonemia was induced by adding 1, 3 or 5 mM NH₄Cl to the culture medium. The hyperammonemic levels induced, which are pathophysiological in nature, are those most commonly employed in *in vitro* experiments. Given that NH₄Cl completely dissociates, the final concentration of ammonia was the same as the NH₄Cl concentration. Culture media were changed every three days, and new NH₄Cl added to maintain stable ammonia concentrations.

Cell number analysis

Detached astroglial cells were reseeded in 24-multiwell plates (12,000 cells/well) with 5% FBS. Three days later these cells were exposed to ammonia (1, 3 or 5 mM NH₄Cl) for 1, 3 or 10 days. Both control and treated cells were then washed with PBS, detached with trypsin, washed again, and centrifuged (100 g for 5 min) in culture medium. After suspension in PBS, the cells were stained with trypan blue to identify those alive and dead; enumerating was performed using a Countess automatic cell counter (Invitrogen) and cell counting chamber slides. The experiment was performed in duplicate with six wells used for each duration and ammonia concentration.

Viability: MTT assay

Astroglial cells were seeded (12,000 cells/well) and grown in 24-well plates, and the experiment begun three days after confluence was reached and the FBS content reduced to 5%. The cells were subjected to 1, 3 and 5 mM of NH₄Cl for 1, 3, 5 and 10 days as above; this was performed in duplicate with 6 wells used for each duration and ammonia concentration. MTT (3-[4,5-dimethylthiazol-2-yl]-2,5-diphenyltetrazolium bromide) was used to assess cell viability. Formazan was solubilized with DMSO and colorimetric analysis performed using a LX800 microplate reader (Biotek Instruments) with 570/630 nm filters.

Cell cycle analysis

The treatments and conditions were the same as above with the exception that the cells were reseeded in 6-multiwell plates (130,000 cells/well), and exposure to ammonia was for a full 10 days. After suspension in PBS, the cells were permeabilized and stained with propidium iodide. Their DNA content was measured using a FACSCalibur flow cytometer (Becton-Dickinson) employing a 488 nm argon ion laser as the excitation source. Cell cycle analysis was performed using Cylchred free software. The experiment was performed in triplicate, with six wells used for each ammonia concentration.

Well DNA content

Cells were grown in 96-multiwell plates and exposed to ammonia as described above for 1, 5 or 10 days. After confluence the cells were fixed in formaldehyde (3% in PBS) for 20 min at room temperature and permeabilized using a solution of 0.1% Triton X-100 in PBS. A solution of DRAQ5 (diluted 1:2000) was used for DNA staining. After five 5 min washes and the complete removal of the wash solution, the plate was immediately scanned at 700 nm using an infrared imaging system (LICOR Biosciences). This experiment was performed only once, but using 20 wells for each duration and ammonia concentration.

BrdU incorporation

The experimental conditions were the same as those described for cell number analysis, although the cells were grown over round coverslips to facilitate the quantification of BrdU incorporation. BrdU (Sigma) (1 $\mu\text{g}/\text{mL}$ for 5 min) was added to the culture medium and incubated at 37°C. For the detection of BrdU, and following 4% paraformaldehyde fixation, the samples were incubated with the appropriate primary antibody (DAKO) (diluted 1:300) at 4°C overnight. An appropriate Cy3-labelled secondary antibody (Jackson) (diluted 1:1500 in blocking solution) was then added and incubation allowed to proceed for 1 h at room temperature. Nucleic acids were stained with DAPI. The stains were analyzed by conventional fluorescence microscopy (Zeiss) or confocal microscopy (Leica SP5). The number of positive cells was recorded as a percentage of the total number.

Effect of ammonia on DNA polymerase

TaqDNA polymerase DNA replication efficiency was measured in real-time polymerase chain reactions (PCR) using Ct as a measure of amplification. Peripheral blood mononuclear cells from a donor were isolated by Ficoll gradient separation and their RNA isolated using the RibozolTM Plus RNA Purification Kit (Amresco). RNA concentrations were measured using a Quawell Q5000 spectrophotometer (Quawell). RNA integrity was verified using the Agilent RNA 6000 Nano Kit and employing a 2100 Bioanalyzer (Agilent). cDNA was generated from 1 μg of total RNA using the High Capacity cDNA Archive Kit (Life Technologies). The final reaction volume was 20 μL . Real-time PCR was performed in triplicate in a MicroAmpTM Fast 96-well reaction plate (0.1 mL) (Life Technologies) using 2 $\mu\text{L}/\text{well}$ of a 1:10 dilution of cDNA plus 0.04 μM of *GAPDH* forward (5'-AGC CAC ATC GCT CAG ACA C-3') and reverse (5'-GCC CAA TAC GAC CAA ATC C-3') primers and 1 \times SYBR Green PCR Master Mix (Roche Applied Science) (total reaction volume 20 μL). PCR reactions were run at increasing concentrations (1, 3 and 5 mM) of NH_4Cl . A control without NH_4Cl or glutamine was used for comparisons. PCR reactions were run in a StepOne PlusTM Real-Time PCR System (Life Technologies). ROX-normalized Ct values for each condition were compared using StepOneTM Software v.2.3 (Life Technologies).

iTRAQ protein analysis

To obtain sufficient protein for analysis, cultures were raised in 75 cm² flasks—three for every condition combination studied (1, 3, 5 and 10 days, with 1, 3 or 5 mM NH₄Cl). The experiment, performed in duplicate, began three days after confluence was reached and the FBS content had been reduced to 5%. Cells were detached and processed according to the Calbiochem Complete Proteo Extract Kit User's Guide, and maintained at -80°C until use.

Cell pellets were dissolved in lysis buffer (8 M urea, 2 M thiourea, 5% CHAPS, 2 mM TCEP-HCl and protease inhibitor) and the cells subjected to ultrasonication (10 pulses at low amplitude) on ice. The lysed product was centrifuged at 20,000 *g* for 10 min at 4°C, and the supernatant containing the solubilized proteins later used in iTRAQ experiments. The total protein concentration was determined using the Pierce 660 nm Protein Assay Kit (Thermo). For digestion, 40 µg of the protein produced by each treatment were precipitated by the methanol/chloroform method. Protein pellets were resuspended and denatured in 20 µl of 7 M urea/2M thiourea/100 mM TEAB, pH 7.5, and reduced with 1 µL of 50 mM Tris(2-carboxyethyl) phosphine (TCEP, AB SCIEX), pH 8.0, at 37°C for 60 min. This was followed by the addition of 2 µL of 200 mM cysteine-blocking reagent (methyl methanethiosulfonate (MMTS) (Pierce) for 10 min at room temperature. Samples were diluted to 140 µL with 25 mM TEAB to reduce the urea/thiourea concentration. Digestions were initiated by adding 2 µL (1 µg/µL) sequence grade-modified trypsin (Sigma-Aldrich) to each sample in the ratio 1:20 (w/w); the reactions were incubated at 37°C overnight on a shaker. The digested samples were then labeled with different iTRAQ tags as follows: control, iTRAQ 114 or 115; celastrol-treated, iTRAQ 116 or 117. The samples were then pooled and dried and the peptides further labeled using the iTRAQ 4-plex Kit (AB SCIEX) according to the manufacturer's instructions. After labeling, the samples were pooled, dried and desalted using a SEP-PAK C18 Cartridge (Waters). Finally, the cleaned tryptic peptides were evaporated to dryness and stored at -20°C until analysis.

A 2 µg aliquot of these pooled, cleaned, tryptic peptides was subjected to 2D-nano LC ESI-MSMS analysis using a nano liquid chromatography system (Eksigent Technologies nanoLC Ultra 1D plus, AB SCIEX) coupled to high speed Triple TOF 5600 mass spectrometer (AB SCIEX) with a duo spray ionization source. The analytical column used was a silica-based reversed phase column (C18 ChromXP, 75 µm × 15 cm, 3 µm particle size, 120 Å pore size) (Eksigent Technologies, AB SCIEX). The trap column was also a C18 ChromXP model, in line with the analytical column. The loading pump delivered a solution of 0.1% formic acid in water at 2 µL/min. The nano-pump provided a flow rate of 300 nL/min and was operated under gradient elution conditions using 0.1% formic acid in water as mobile phase A, and 0.1% formic acid in acetonitrile as mobile phase B. Peptides with iTRAQ labels were separated using a 200 min gradient ranging from 2% to 90% mobile phase B (mobile phase A: 2% acetonitrile, 0.1% formic acid; mobile phase B: 100% acetonitrile, 0.1% formic acid). The injection volume was 5 µL.

Data were acquired using a TripleTOF 5600 System (AB SCIEX) with the following settings: ion spray voltage floating (ISVF) 2800 V, curtain gas (CUR) 20 l/h, interface heater temperature (IHT) 150°C, ion source gas 1 (GS1) 20 l/h, declustering potential (DP) 85 V. All data were collected in information-dependent acquisition (IDA) mode using Analyst TF 1.5 software (AB SCIEX). A 0.25 s MS survey scan was performed in the mass range 350–1250 Da, followed by 30 MS/MS scans of 150 ms in the mass range 100–1800 (total cycle time: 4.04 s). Switching criteria were set to ions with a mass/charge ratio (*m/z*) of >350 but <1250, with a charge state of 2–5 and an abundance threshold of more than 70 counts (cps). Former target ions were excluded for 20 s. The IDA rolling collision energy (CE) parameters script option was used for automatically controlling the CE.

MS and MS/MS data obtained for pooled samples were processed using Analyst[®] TF 1.5.1 software (AB SCIEX). Raw data file conversion tools generated mgf files which were compared against the *Homo sapiens* database (which contains 40,530 protein-coding genes and their corresponding reversed entries), using the Mascot Server v. 2.5.0 (Matrix Science). The search parameters were: enzyme, trypsin; allowed missed cleavages, 1; fixed modifications, iTRAQ4-plex (N-term and K) and beta-methylthiolation of cysteine; variable modifications, oxidation of methionine. Peptide mass tolerance was set at ± 25 ppm for precursors and 0.05 Da for fragment masses. The confidence interval for protein identification was set to $\geq 95\%$ ($p < 0.05$); only peptides with an individual ion score above the 1% false discovery rate (FDR) threshold were considered correctly identified. Only proteins with at least two quantified peptides were considered in quantitation. A 5% quantitation FDR threshold was used to consider proteins differentially expressed.

Statistical analysis

One-way ANOVA followed by a Bonferroni post-hoc comparison for pairwise tests was used to compare the measured variables between control and treatment cultures. Only significant changes between the control and ammonia-treated groups are included in the figures; significant changes between different ammonia-treated groups are not included.

Results

To determine the optimum conditions for studying changes in the proliferative activity of the cells, a preliminary experiment was performed. It is logical to assume that cells growing under very low FBS content conditions might have a low proliferative rate, and that this might make it difficult to detect any effect of ammonia. Confluent astroglial cells were exposed to 5 mM NH_4Cl for 10 days with either 0.5 or 5% FBS. [Fig 1](#) shows that ammonia affects astroglial proliferation, but this effect was only clear for the cells cultured with 5% FBS: a significant 40% reduction ($p < 0.01$) was detected with 5% FBS, but only a non-significant 20% reduction was observed in cells growing with 0.5% FBS.

Cell number analysis and viability

Exposure to ammonia induced a dose- and time-dependent reduction in cell number. Clear, significant reductions were observed after 10 days in the 3 and 5 mM ammonia treatments (44.8 and 50.4% respectively; $p < 0.01$) ([Fig 2](#)). These reductions were not due to an increase in the number of dead cells; their number was small and very similar under all experimental condition (data not shown).

The MTT assay showed ammonia to affect cell viability in a dose- and time-dependent manner ([Fig 3](#)). A 40% reduction in viability was detected after 10 days of exposure to 5 mM ammonia, a reduction reflected in the cell count analysis. Indeed, a strong correlation was seen between the cell count ([Fig 2](#)) and viability data ([Fig 3](#)) ($r = 0.933$, $p = 0.51 \times 10^{-4}$).

Cell cycle analysis

No significant differences were observed between treatments in terms of the number of cells in the G_2 -M phase. However, a clear increase in the number of cells in the S phase was detected (reaching 9% with the 5 mM ammonia treatment), with a concomitant reduction in the number of cells in the G_0 - G_1 phase ([Fig 4](#)). Using the algorithm $N = N_0 \times 2^{t/g}$ (where N and N_0 are the final and initial cell numbers, t the duration of treatment, and g the duration of the cell cycle), and taking into account (1) a cell cycle length 20 h [[12](#)], (2) 10 days of exposure, and (3)

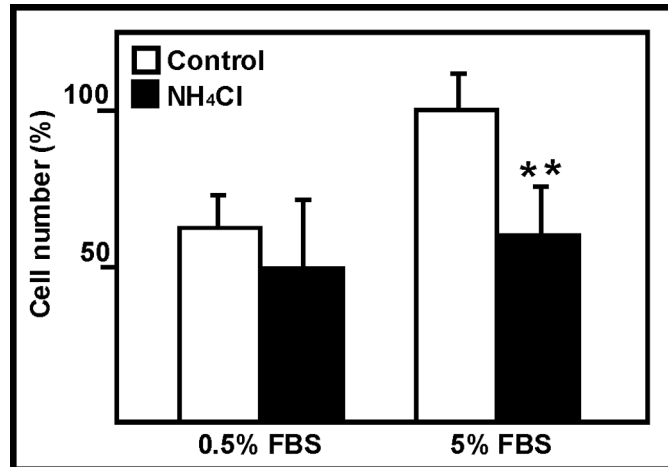


Fig 1. Effect of ammonia and serum on astroglial proliferation. Effect of ammonia (NH₄Cl) exposure on astroglial proliferation was tested at two FBS concentrations (0.5 and 5%). **p<0.01. The percentage value is calculated taking the value for the 5% FBS control as 100% (1.65 x 10⁵ cells). Columns and bars represent means and SDs.

doi:10.1371/journal.pone.0139619.g001

that ammonia induces a 10% time delay in the completion of the cell cycle, a theoretical reduction of 46% is obtained. This figure lies between the 40% and 50% reductions detected in cell count analysis.

Well DNA content

A lower cell proliferation rate leads to a reduction in cell number, which should be associated with a lower well DNA content. This was measured using an in-cell based assay to avoid protocols including cell fragmentation and DNA extraction. In general, the well DNA content was

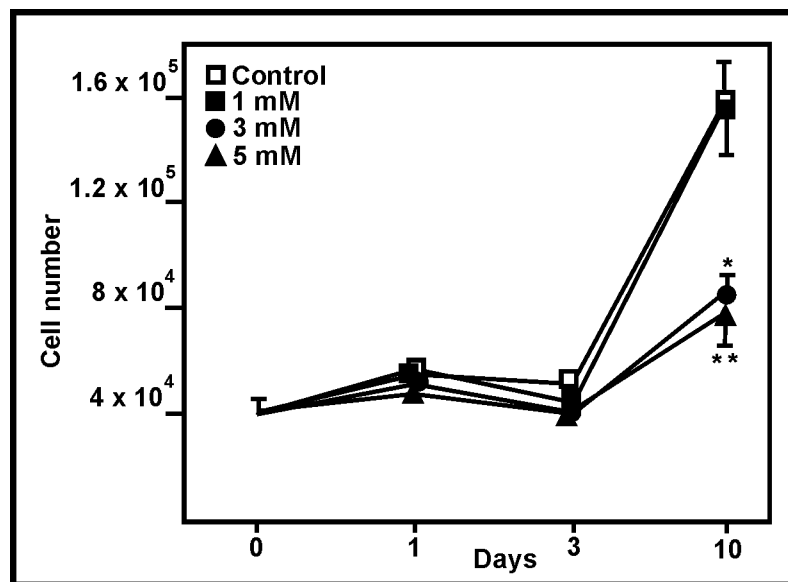


Fig 2. Effect of ammonia on astroglial proliferation. Change in astroglial cell number after 10 days of exposure to ammonia. Standard deviations are not shown for 1 and 3 days since differences between the control and ammonia-treated cells were not significant at these times. *p<0.05, **p<0.01.

doi:10.1371/journal.pone.0139619.g002

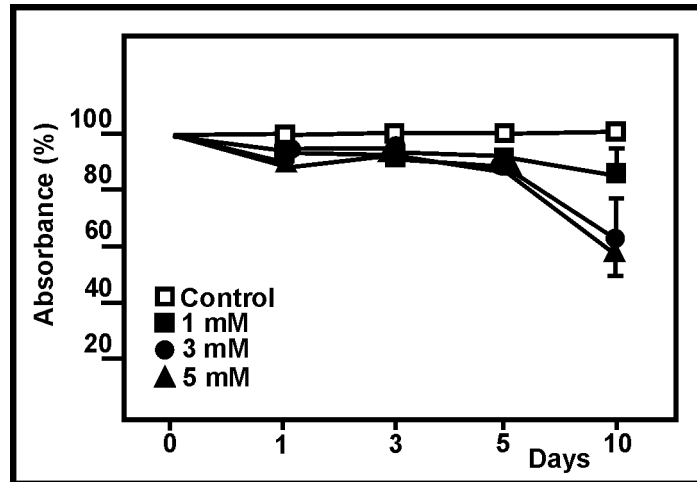


Fig 3. Effect of ammonia on viability of astroglial cells. MTT viability assay of astroglial cells exposed to ammonia. Points and bars represent means and SDs. No SD values are included for 1, 3 and 5 days since they were <10% different to the mean.

doi:10.1371/journal.pone.0139619.g003

reduced when cells were treated with ammonia, with significant changes observed after 5 days of exposure to the 5 mM concentration, and after 10 days of exposure to the 3 mM concentration (Fig 5).

BrdU incorporation

The delay in the completion of the S phase was examined by BrdU incorporation. BrdU is incorporated into newly synthesized DNA in the place of thymidine, and is very easy to detect; slower DNA synthesis should thus be revealed by reduced BrdU incorporation. BrdU was incorporated to a lesser extent by ammonia-treated than by control cells (Fig 6). At 10 days,

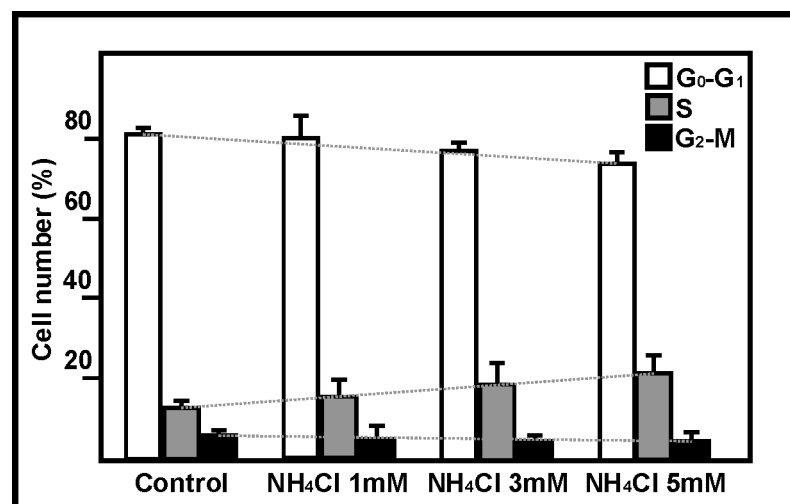


Fig 4. Effect of ammonia on cell cycle phases. Cell cycle analysis after 10 days of exposure to 1, 3 and 5 mM ammonia. The dotted lines are included to indicate the trends for the cell cycle phases. Columns and bars represent means and SDs. The percentages of cells in the phases considered (G₀-G₁, S and G₂-M) are included for every experimental condition; it should be noted that the sum of the three phases is 100% (10⁴ cells).

doi:10.1371/journal.pone.0139619.g004

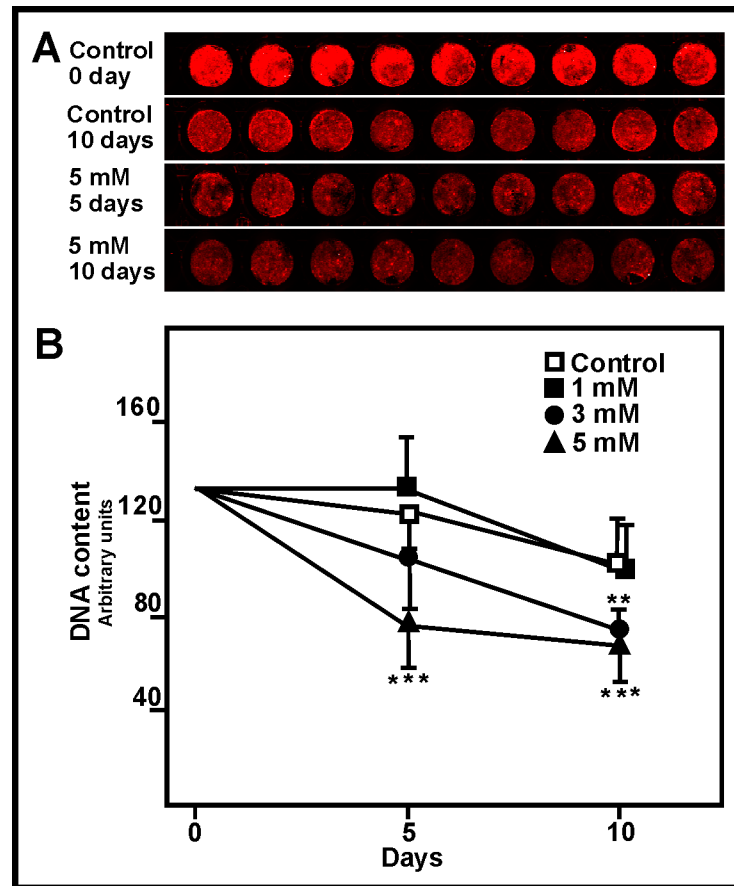


Fig 5. Effect of ammonia on DNA content. (A) Four rows of the in-cell DNA content analysis plate; note that ammonia exposure reduced the fluorescence signal. The row shows only nine results since the external wells were not seeded and the control point without fluorescent dye is not included. (B) Plot showing the change in well DNA content after ammonia exposure. Points and bars represent means and SDs. ** $p < 0.05$, *** $p < 0.01$.

doi:10.1371/journal.pone.0139619.g005

the 5 mM ammonia-treated cells incorporated 45.5% less BrdU than did controls, in line with the reduction recorded in cell count analysis.

Effect of ammonia on DNA polymerase

To determine whether the delay in DNA synthesis was due to an ammonia dysfunction involving DNA polymerase, real-time PCR analysis starting with the same quantity of cDNA was performed with or without ammonia in the reaction medium. Fig 7 shows that ammonia had no significant effect on DNA amplification or, consequently, on DNA polymerase function. Given that a difference of 1 unit in Ct corresponds to a 2x-fold expression change, the differences observed under the different ammonia conditions are extremely small.

iTRAQ protein analysis

Table 1 shows that the expression of histones H1, H2A, H2B, H3 and H4, and of heterochromatin protein 1 (HP1, a non-histone chromatin protein), was reduced by exposure to ammonia in a dose-dependent manner.

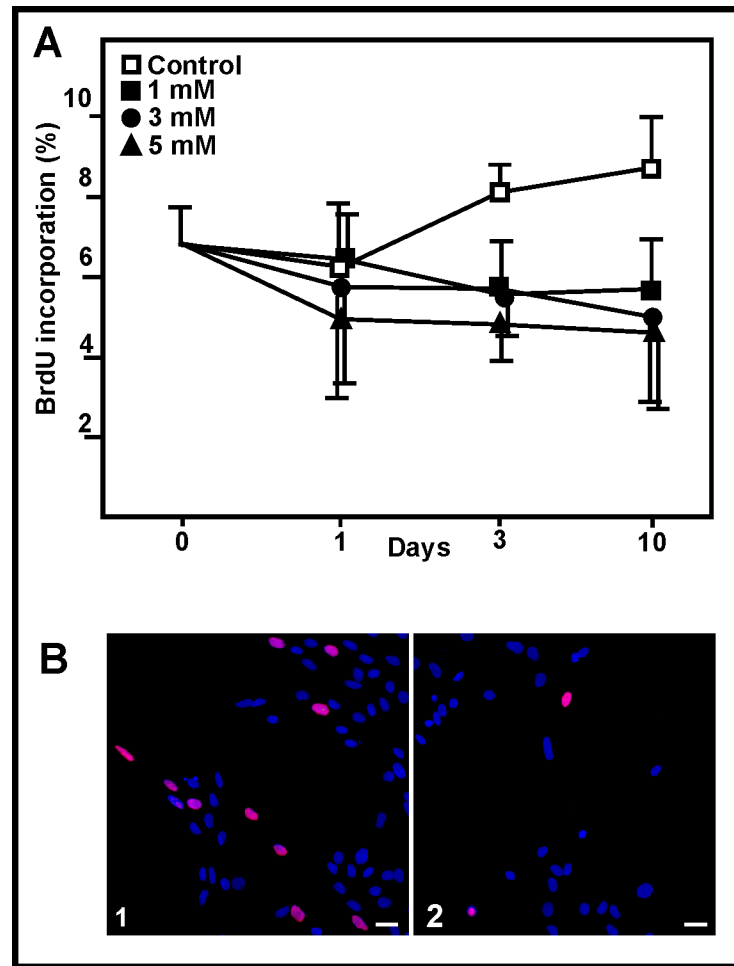


Fig 6. Effect of ammonia on BrdU incorporation. (A) BrdU incorporation by astroglial cells following exposure to ammonia. Points and bars represent means and SD. No significant changes were observed. (B) Cultured cells showing BrdU incorporation (red): (1) 1 day control, (2) 3 days after exposure to 5 mM ammonia. Scale bar: 10 μ m.

doi:10.1371/journal.pone.0139619.g006

Discussion

The effect of ammonia on cell proliferation has been studied in enterocytes, kidney epithelial cells and nerve cells, but information regarding its effect on cell proliferation in astroglia is very scarce, and what there is can be contradictory. In general, ammonia inhibits cell proliferation; this has been reported for human gastric cancer cells (HGC-27, MKN-1 and MKN-45) [13, 14], human colon adenocarcinoma cells (HF-29) [15], and human prostatic cancer cells (DU-145) [16]. However, contradictory results were obtained in the first autoradiographic studies: a dose-dependent depression of cell replication was seen in cultured kidney cells [17] yet no influence on proliferation was observed in rat enterocytes (IEL-6 line) [18]. The first studies on the effect of ammonia in *in vivo* models suggested there to be an increase in astroglial proliferation [9,10]. In fact, DNA synthesis has been shown in Alzheimer type II astrocytes, a cell type that appears in HE [19]. However, the results of the present work show that ammonia reduces the proliferative activity of astroglial cells in culture. Similar inhibition has been reported for astrocytoma cells [20] and cultured astrocytes [21]. The fact that increased and decreased proliferative activity has been described in *in vivo* and *in vitro* models respectively may reflect

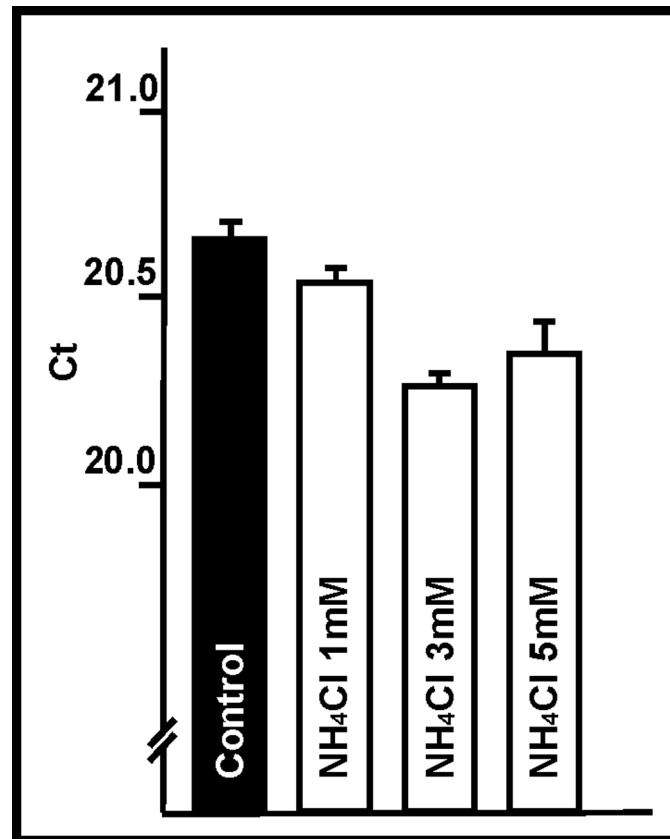


Fig 7. Effect of ammonia on DNA polymerase. Effect of ammonia (NH₄Cl) on the activity of DNA polymerase, analyzed via real-time PCR. Note that the Ct variation ranges between 20 and 21. Columns and bars represent means and SDs. No significant changes were observed.

doi:10.1371/journal.pone.0139619.g007

differences in these models themselves; moreover, it should be remembered that *in vitro* models cannot fully reproduce HE. It is well known that astroglial cells proliferate in the adult central nervous system and that this proliferative activity may be involved in the development of different cognitive functions. HE causes, among other neurological disorders, the impairment of memory formation [22], and astrocytes have been clearly involved in establishing memory [23]. Thus, it might be that a reduction in astroglial proliferation is involved in the memory and cognitive alterations seen in HE [24, 25].

Table 1. iTRAQ analysis of histones and HP1 expression.

		H1	H2A	H2B	H3	H4	HP1
1 mM NH ₄ Cl	p-value	0.012	0.038	0.402	0.05	0.007	0.11
	z-score	-2.50	-2.06	-0.83	-1.95	-2.69	-1.59
3 mM NH ₄ Cl	p-value	0.05	0.005	0.067	0.028	0.009	0.022
	z-score	-1.88	-2.60	-1.82	-2.18	-2.58	-2.28
5 mM NH ₄ Cl	p-value	1.3 10 ⁻⁵	4.2 10 ⁻⁵	0.03	6.5 10 ⁻⁴	1.1 10 ⁻⁴	0.005
	z-score	-4.34	-3.00	-2.08	-3.40	-3.86	-2.79

Change in p-value and z-score for histones (H1, H2A, H2B, H3 and H4) and HP1 determined by iTRAQ analysis of astroglial cells exposed to ammonia for 5 days.

doi:10.1371/journal.pone.0139619.t001

A number of mechanisms have been proposed to explain the inhibition of cell proliferation from a cell cycle perspective. The accumulation of cells in the S [14] or G₂-M [26] phases in ammonia-treated cells has been reported, but so has the repression of proliferation with no changes in the distribution of cells in the different phases of the cell cycle [15]. The inhibitory effect of ammonia on the synthesis of polyamines (metabolites needed for cell growth) has been proposed responsible for the latter. The present results, and those of Matsui et al. [14] in enterocytes, clearly show that exposure to ammonia causes astroglial cells to become delayed in the S phase. This might increase the length of the cell cycle by 10%, enough to explain the inhibition of proliferation observed in the present work. The possibility that ammonia might inhibit entry into the cell cycle has also been suggested; indeed, the p53-mediated enhanced transcription of cell cycle inhibitory genes (GADD45 α and p21) in the presence of ammonia has recently been demonstrated [21]. The inhibition of cell cycle entry by ammonia [21], and the induction of cell cycle delay (present results) are not mutually exclusive processes. On the contrary, they should be considered complementary strategies aimed at reducing astroglial proliferation.

The synthesis of chromatin is a pivotal event in the S phase. Chromatin is composed of DNA and specific proteins, and the synthesis of both is finely regulated; in fact, an imbalanced synthesis compromises chromosome replication. The present results show that ammonia inhibits DNA synthesis, as indicated by the reduced DNA content and BrdU incorporation observed in the ammonia-treated cells. A similar inhibitory effect of ammonia on DNA synthesis has been reported in other studies [14, 17, 27]. Neither BrdU incorporation nor mitotic figures were observed in the liver of rats in an *in vivo* model of fulminant hepatic failure associated with hyperammonemia [28]. However, DNA synthesis and mitotic divisions have been described in Alzheimer type II astrocytes, cells associated with HE [19]. To determine whether the inhibition of DNA synthesis was due to an effect of ammonia and/or glutamine on DNA polymerase, the functioning of this enzyme under high ammonia concentrations was tested using PCR. No significant changes in the enzyme's functioning were seen; it seems that DNA polymerase is not affected by ammonia.

A reduction in DNA synthesis should be associated with an inhibition in chromatin protein expression. The present results are the first to reveal an inhibitory effect of ammonia on the expression of histones H1, H2A, H2B, H3 and H4, and HP1. The present results cannot, of course, reveal whether the inhibition of DNA synthesis is the cause or the effect of the inhibition of chromatin protein expression. However, it is well known that most histone proteins are produced during the S phase, and that their synthesis depends on DNA replication. In fact, these histones are known as replication-dependent proteins [29]. Thus, the inhibition of DNA synthesis by ammonia ought to inhibit histone synthesis. HP1 is a non-histone chromosomal protein associated with heterochromatin; it is essential for maintaining the active transcription of genes involved in cell cycle progression [30].

It is well known that energy metabolism influences the progression of the cell cycle, and that ammonia affects the metabolic status of the cell. Thus, the effect of ammonia on astroglial proliferation might be due to an energy imbalance. However, the results show that exposure to ammonia greatly reduced cell viability, and that this correlated strongly with the reduction in cell number. This suggests that the loss of viability is almost exclusively due to the reduction in cell number and not to alterations in energy metabolism. The possibility that the loss of viability is owed to cell death can be ruled out since the number of dead cells was very low and similar under all experimental conditions. Although a clear inhibitory effect of ammonia leading to mitochondrial dysfunction has been observed in different studies [31, 32], the effects of ammonia on cerebral oxidative energy metabolism are heterogeneous [33]. Certainly, the role of astroglial cells in cerebral oxidative metabolism remains somewhat unclear. Mitochondrial

dysfunction induced by changes in mitochondrial permeability transition [34], and in the malate-aspartate shuttle [35], have been observed in *in vitro* studies, but no changes in astroglial oxidative metabolism have been seen in *in vivo* studies [36]. The present iTRAQ results confirm that ammonia induces alterations in astroglial energy metabolism, but the response is positively regulated, as suggested by the significant increase detected in many mitochondrial proteins, including ADP/ATP translocase, mitochondrial import receptor subunit TOM6, and ATP synthetase subunit δ (z-score 3.11, 2.54, and 1.8 respectively). The possibility that these changes represent an adaptive response to ammonia-induced alterations in mitochondrial metabolism of astrocytes needs to be investigated.

Conclusions

Ammonia induces a dose- and time-dependent reduction in the proliferative activity of astroglial cells in culture. The cell cycle phase analysis and BrdU incorporation results show this reduction to be due to an accumulation of cells in the S phase, as corroborated by a reduced well DNA content and the strong inhibition of the expression of histones and HP1. The interference of energy status by ammonia as a reason for reduced proliferation is not supported. An effect of ammonia and glutamine on DNA polymerase, the enzyme that replicates DNA, does not seem probable, although it cannot be completely ruled out. Further studies are required to determine the precise mechanisms by which ammonia affects DNA synthesis.

Supporting Information

S1 Checklist. ARRIVE checklist.
(DOCX)

Acknowledgments

We thank Dr. Fernando San Segundo of the Dept. of Physics and Mathematics (University of Alcalá de Henares), for assistance with the statistical analyses.

Author Contributions

Conceived and designed the experiments: GB BS SC LALF IT. Performed the experiments: GB BS SC MCM LALF MIG IT. Analyzed the data: GB BS SC MCM LALF MIG IT. Wrote the paper: GB BS SC LALF IT IS.

References

1. Butterworth RF, Giguère JF, Michaud J, Lavoie J, Layrargues GP. Ammonia: key factor in the pathogenesis of hepatic encephalopathy. *Neurochem Pathol.* 1987; 6: 1–12.
2. Bosoi CR, Rose CF. Identifying the direct effects of ammonia on the brain. *Metab Brain Dis.* 2009; 24: 95–102. doi: [10.1007/s11011-008-9112-7](https://doi.org/10.1007/s11011-008-9112-7) PMID: [19104924](https://pubmed.ncbi.nlm.nih.gov/19104924/)
3. Häussinger D, Schliess F. Pathogenetic mechanisms of hepatic encephalopathy. *Gut.* 2008; 57: 1156–1165. doi: [10.1136/gut.2007.122176](https://doi.org/10.1136/gut.2007.122176) PMID: [18628377](https://pubmed.ncbi.nlm.nih.gov/18628377/)
4. Ott P, Vilstrup H. Cerebral effects of ammonia in liver disease: current hypotheses. *Metab Brain Dis.* 2014; 29: 901–911. doi: [10.1007/s11011-014-9494-7](https://doi.org/10.1007/s11011-014-9494-7) PMID: [24488230](https://pubmed.ncbi.nlm.nih.gov/24488230/)
5. Norenberg MD. The role of astrocytes in hepatic encephalopathy. *Neurochem Pathol.* 1987; 6: 13–33. PMID: [3306480](https://pubmed.ncbi.nlm.nih.gov/3306480/)
6. Norenberg MD, Martínez-Hernández A. Fine structural localization of glutamine synthetase in astrocytes of rat brain. *Brain Res.* 1979; 161: 303–310. PMID: [31966](https://pubmed.ncbi.nlm.nih.gov/31966/)
7. Albrecht J. Astrocytes in ammonia neurotoxicity: A target, a mediator and a shield. In: Aschner M, Costa LG, editors. *The Role of Glia in Neurotoxicity.* Boca Raton: CRC Press; 2005. pp. 329–342.

8. Rama Rao KV, Norenberg MD. Aquaporin-4 in hepatic encephalopathy. *Metab Brain Dis.* 2007; 22: 265–275. PMID: [17879149](#)
9. Norenberg MD, Lapham LW, Eastland ME, May AG. Division of protoplasmic astrocytes in acute experimental hepatic encephalopathy. An electron microscopy study. *Am J Pathol.* 1972; 67: 403–408. PMID: [5021108](#)
10. Diemer NH, Laursen H. Glial cell reactions in rats with hyperammonemia induced by urease or portocaval anastomosis. *Acta Neurol Scand.* 1977; 55: 425–442. PMID: [878834](#)
11. Bodega G, Suárez I, López-Fernández LA, Almonacid L, Zaballos A, Fernández B. Possible implication of ciliary neurotrophic factor (CNTF) and β -synuclein in the ammonia effect on rat astroglial cells in culture. A study using DNA and protein microarrays. *Neurochem Int.* 2006; 48: 729–738. PMID: [16483693](#)
12. Knapp PE. The cell cycle of glial cells grown in vitro: an immunocytochemical method of analysis. *J Histochem Cytochem.* 1992; 40: 1405–1411. PMID: [1506676](#)
13. Matsui T, Matuskawa Y, Sakai T, Nakamura K, Aoike A, Kawai K. Effect of ammonia on cell-cycle progression of human gastric cancer cells. *Eur J Gastroen Hepatol.* 1995; 7 (Suppl. 1): S79–S81.
14. Matsui T, Matuskawa Y, Sakai T, Nakamura K, Aoike A, Kawai K. Ammonia inhibits proliferation and cell cycle progression at S-phase in human gastric cells. *Digest Dis Sci.* 1997; 42: 1394–1399. PMID: [9246035](#)
15. Mouillé B, Delpal S, Mayeur C, Blachier F. Inhibition of human colon carcinoma cell growth by ammonia: a non-cytotoxic process associated with polyamine synthesis reduction. *BBA-Gen Subjects.* 2003; 1624: 88–97.
16. Won JH, Parekattil SJ, Davidson SD, Luddy JS, Choudhury MS, Mallouh C, et al. Ammonium-chloride-induced prostatic hypertrophy in vitro: urinary ammonia as a potential risk factor for benign prostatic hyperplasia. *Urol Res.* 1999; 27: 376–381. PMID: [10550527](#)
17. Rabkin R, Palathumpat M, Tsao T. Ammonium chloride alters renal tubular cell growth and protein turnover. *Lab Invest.* 1993; 68: 427–438. PMID: [8479151](#)
18. Zachrisson K, Midtvedt T, Uribe A. The in vitro effect of ammonia on DNA synthesis in rat enterocytes. *Eur J Gastroen Hepatol.* 1994; 6: 951–954.
19. Brumback RA, Lapham LW. DNA synthesis in Alzheimer type II astrocytosis. The question of astrocytic proliferation and mitosis in experimentally induced hepatic encephalopathy. *Arch Neurol.* 1989; 46: 845–848. PMID: [2757524](#)
20. Hillmann P, Köse M, Söhl K, Müller CE. Ammonium-induced calcium mobilization in 1321N1 astrocytoma cells. *Toxicol Appl Pharm.* 2008; 227: 36–47.
21. Görg B, Karababa A, Shafiqulina A, Bidmon HJ, Häussinger D. Ammonia-induced senescence in cultured rat astrocytes and in human cerebral cortex in hepatic encephalopathy. *Glia.* 2015; 63: 37–50. doi: [10.1002/glia.22731](#) PMID: [25092802](#)
22. Leke R, Oliveira DL, Forgiarini LF, Escobar TD, Hammes TO, Meyer FS, et al. Impairment of short term memory in rats with hepatic encephalopathy due to bile duct ligation. *Metab Brain Dis.* 2013; 28: 187–192. doi: [10.1007/s11011-012-9347-1](#) PMID: [23111918](#)
23. Santello M, Volterra A. Astrocytes as aide-mémoires. *Nature.* 2010; 463: 169–170. doi: [10.1038/463169a](#) PMID: [20075911](#)
24. Weissenborn K, Giewekemeyer K, Heidenreich S, Bokemeyer M, Berding G, Ahl B. Attention, memory, and cognitive function in hepatic encephalopathy. *Metab Brain Dis.* 2005; 20: 359–367. PMID: [16382346](#)
25. Méndez M, Méndez-López M, López L, Aller MA, Arias J, Arias JL. Associative learning deficit in two experimental models of hepatic encephalopathy. *Behav Brain Res.* 2009; 198: 346–351. doi: [10.1016/j.bbr.2008.11.015](#) PMID: [19056427](#)
26. Renau-Piqueras J, O'Connor JE, Báguena-Cervellera R, Grisolia S. Ammonium chloride-induced alterations in growth kinetics and ultrastructure of murine neuroblastoma cells. A flow cytometric and stereologic analysis. *Virchows Arch B Cell Pathol Incl Mol Pathol.* 1986; 50: 271–283. PMID: [2870578](#)
27. Franch HA. Modification of the epidermal growth factor response by ammonia in renal cell hypertrophy. *J Am Soc Nephrol.* 2000; 11: 1631–1638. PMID: [10966487](#)
28. Eguchi S, Kamlot A, Ljubimova J, Hewitt WR, Lebow LT, Demetriou AA, et al. Fulminant hepatic failure in rats: survival and effect on blood chemistry and liver regeneration. *Hepatology.* 1996; 24: 1452–1459. PMID: [8938180](#)
29. Rattray AMJ, Müller B. The control of histone gene expression. *Biochem Soc Trans.* 2013; 40: 880–885.
30. De Lucia F, Ni J-Q, Vaillant C, Sun F-L. HP1 modulates the transcription of cell cycle regulators in *Drosophila melanogaster*. *Nucl Acids Res.* 2005; 33: 2852–2858. PMID: [15905474](#)

31. Bjerring PN, Larsen FS. Changes in cerebral oxidative metabolism in patients with acute liver failure. *Metab Brain Dis.* 2013; 28: 179–182. doi: [10.1007/s11011-012-9346-2](https://doi.org/10.1007/s11011-012-9346-2) PMID: [23099996](https://pubmed.ncbi.nlm.nih.gov/23099996/)
32. Rama Rao KV, Norenberg MD. Cerebral energy metabolism in hepatic encephalopathy and hyperammonemia. *Metab Brain Dis.* 2001; 16: 67–78. PMID: [11726090](https://pubmed.ncbi.nlm.nih.gov/11726090/)
33. Schousboe A, Waagepetersen HS, Leke R, Bak LK. Effects of hyperammonemia on brain energy metabolism: controversial findings in vivo and in vitro. *Metab Brain Dis.* 2014; 29: 913–917. doi: [10.1007/s11011-014-9513-8](https://doi.org/10.1007/s11011-014-9513-8) PMID: [24577633](https://pubmed.ncbi.nlm.nih.gov/24577633/)
34. Rama Rao KV, Jayakumar AR, Norenberg DM. Ammonia neurotoxicity: role of the mitochondrial permeability transition. *Metab Brain Dis.* 2003; 18: 113–127. PMID: [12822830](https://pubmed.ncbi.nlm.nih.gov/12822830/)
35. Kala G, Hertz L. Ammonia effects on pyruvate/lactate production in astrocytes—Interaction with glutamate. *Neurochem Int.* 2005; 47: 4–12. PMID: [15890434](https://pubmed.ncbi.nlm.nih.gov/15890434/)
36. Iversen P, Mouridsen K, Hansen MB, Jensen SB, Sørensen M, Bak LK, et al. Oxidative metabolism of astrocytes is not reduced in hepatic encephalopathy: a PET study with [¹¹C]acetate in humans. *Front Neurosci.* 2014; 8:353.